Journal of Applied Polymer Science

Zwitterionic-polymer-functionalized poly(vinyl alcohol-*co*-ethylene) nanofiber membrane for resistance to the adsorption of bacteria and protein

Wenwen Wang, Ying Lu, Mengying Luo, Qinghua Zhao, Yuedan Wang, Qiongzhen Liu, Mufang Li, Dong Wang

School of Materials Science and Engineering, Wuhan Textile University, Wuhan 430200, China

Correspondence to: D. Wang (E-mail: wangdon08@126.com)

ABSTRACT: A zwitterionic poly(vinyl alcohol-*co*-ethylene) (PVA-*co*-PE) nanofiber membrane for resistance to bacteria and protein adsorption was fabricated by the atom transfer radical polymerization of sulfobetaine methacrylate (SBMA). The PVA-*co*-PE nanofiber membrane was first surface-activated by α-bromoisobutyryl bromide, and then, zwitterionic SBMA was initiated to polymerize onto the surface of nanofiber membrane. The chemical structures of the functionalized PVA-*co*-PE nanofiber membranes were confirmed by attenuated total reflectance–Fourier transform infrared spectroscopy and X-ray photoelectron spectroscopy. The morphologies of the PVA-*co*-PE nanofiber membranes were characterized by scanning electron microscopy. The results show that the poly(sulfobetaine methacrylate) (PSBMA) was successfully grafted onto the PVA-*co*-PE nanofiber membrane, and the surface of the nanofiber membrane was more hydrophilic than that of the pristine membrane. Furthermore, the antibacterial adsorption properties and resistance to protein adsorption of the surface were investigated. This indicated that the PSBMA-functionalized surface possessed good antibacterial adsorption activity and resistance to nonspecific protein adsorption. Therefore, this study afforded a convenient and promising method for preparing a new kind of soft and nonwoven dressing material with antibacterial adsorption and antifouling properties that has potential use in the medical field. © 2016 Wiley Periodicals, Inc. J. Appl. Polym. Sci. **2016**, *133*, 44169.

KEYWORDS: adsorption; grafting; membranes; properties and characterization; surfaces and interfaces

Received 16 March 2016; accepted 6 July 2016

DOI: 10.1002/app.44169

INTRODUCTION

Polymers have been widely used in biomedical fields as implant materials, tissue engineering scaffolds, blood-contacting devices, and disposable clinical apparatus.[1–3] However, it is generally known that the failure of these biomedical devices is usually caused by microbial adhesion onto the implanted biomaterials and the subsequent formation of biofilms.[4,5] Moreover, the adsorption of protein on biomaterials is thought to result in undesired bioreactions and bioresponses; this induces platelet adhesion and the formation of thrombi.[6,7] Therefore, the development of antibacterial and antifouling materials and surfaces is critical in the fields of biomaterials and biosensors.

To date, zwitterions have been widely studied for their antifouling and protein-resistance properties and their antibacterial properties.[8,9] Both inorganic and organic substrates have been modified by zwitterions, and different kinds of materials have been investigated. Colilla *et al.*[10] synthesized a novel zwitterionic SBA-15 (mesoporous silica) type bioceramic with dual antibacterial capability, and this bioceramic was capable of inhibiting 99.9% of bacterial adhesion compared to pure silica SBA-15. In addition, a siloxane sulfopropylbetaine-modified glass surface was prepared; it could kill 99.96% of both *Staphylococcus aureus* and *Escherichia coli* organisms within 24 h.[11] Chen *et al.*[12] reported an approach for the preparation of zwitterionic polyurethanes; this provided another method for integrating integrate antimicrobial and nonfouling properties. Sulfobetaine methacrylate {SBMA; also known as [2-(methacryloyloxy) ethyl] dimethyl-(3-sulfopropyl) ammonium hydroxide} and sulfobetaine methacrylamide (SBMAm) as typical zwitterionic species were surface-initiated by atom transfer radical polymerization (ATRP) from membranes, such as poly(vinylidene difluoride) and polypropylene membranes, to form polymer brushes that could exhibit excellent antibacterial and antifouling properties.[13–15] Furthermore, silver-zwitterion organic–inorganic nanocomposites with antimicrobial and antiadhesive capabilities were synthesized by Li *et al.*,[16] and the obtained CB-Ag hybrid organic–inorganic nanocomposites were able to kill more than 99.8% of *E. coli* K12 in 1 h and release more than 98.7% of dead bacterial cells from the surface.

Hydrophilic poly(vinyl alcohol-*co*-ethylene) (PVA-*co*-PE) nanofiber membranes possess a large specific surface area and can provide abundant hydroxyl groups; these can be widely used in biomaterials, filter substrate, and other applications.[17–21] In this study, we demonstrated the synthesis of poly(sulfobetaine methacrylate) (PSBMA)-functionalized PVA-*co*-PE nanofiber membranes by ATRP to fabricate a surface with both antibacterial adsorption properties and resistance to nonspecific protein adsorption. First, α-bromoisobutyryl bromide (BIBB) was grafted onto the surface of PVA-*co*-PE nanofiber membranes, and then, SBMA was polymerized to form PSBMA brushes on the surface. The surface topography, wettability, surface structures and surface element content were characterized by scanning electron microscopy (SEM), water contact angle measurement, attenuated total reflectance (ATR)–Fourier transform infrared (FTIR) spectroscopy, and X-ray photoelectron spectroscopy (XPS), respectively. The antibacterial properties to microorganisms were measured by a revised absorption method, and the resistance to the nonspecific adsorption of protein was tested by the bicinchoninic acid (BCA) method.

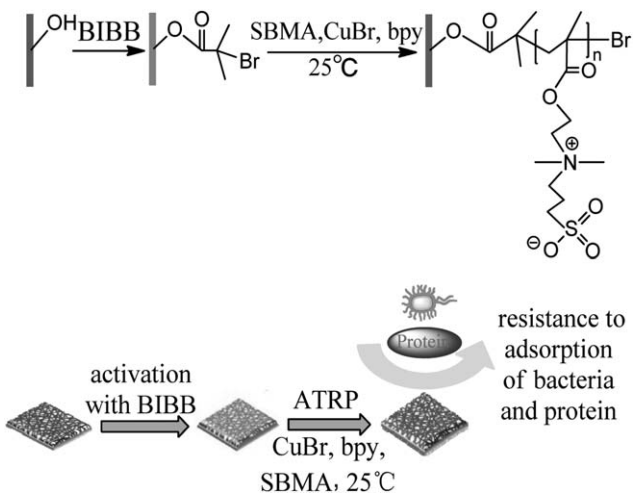

Scheme 1. Fabrication of the zwitterionic polymer-functionalized PVA-*co*-PE nanofiber membrane by ATRP for resistance to bacterial and protein adsorption.

EXPERIMENTAL

Materials

Cellulose acetate butyrate (CAB; butyryl content = 35–39 wt %) was purchased from Acros Chemical. PVA-*co*-PE (ethylene content = 44 mol %) and SBMA (97%) were purchased from Sigma-Aldrich. BIBB (98%), cuprous bromide (CuBr; 99%), 2,2′-bipyridine (bpy; 99%), and bovine serum albumin (BSA; 96%) were supplied by Aladdin (Shanghai, China). Yeast extract and tryptone were purchased from Oxoid. The protein concentration was measured with a BCA assay kit from Sigma. Toluene and methanol were purchased from Sinopharm Chemical Reagent Co., Ltd. Plain polyamide 6 (PA6) woven fabric (120 g/m^2 was purchased from Wujiang Guangjie Textile Co., Ltd. Deionized water and other reagents were used as received.

Preparation of the PVA-*co*-PE Nanofiber Membranes

PVA-*co*-PE nanofibers were prepared according to a previously published procedure.[22] In a typical procedure, mixtures of CAB/PVA-*co*-PE powders with a blend ratio of 80/20 were gravimetrically fed into a corotating twin-screw extruder (Chengrand Research Institute of Chemical Industry, China National BlueStar Co., Ltd.) with an 18-mm screw diameter. The melt extrudates were hot-drawn at the die exit by a take-up device, with the draw ratio kept at 20–25 (the area of the cross section of the die to the extrudate), and air-cooled to room temperature. We prepared the PVA-*co*-PE nanofibers yarns by taking off the CAB matrix from the composite CAB/PVA-*co*-PE fibers via Soxhlet extraction in acetone for 48 h. The technique used for preparing the PVA-*co*-PE nanofiber membranes was reported elsewhere.[23] The typical procedure for preparing the nanofiber membranes was as follows. PVA-*co*-PE nanofibers were dispersed in an aqueous solution with a high-speed shear mixer at 8000 rpm to form a stable aqueous suspension. The suspension was then coated with a high-pressure airflow molding method onto the surface of the PA6 substrates (120 g/m^2 woven fabric) to form a nanofibrous membrane (PA6/nanofiber). Then, the nanofibrous membrane with substrate was dried at room temperature and stored for use.

Binding of the ATRP Initiator onto the Surface of the PVA-*co*-PE Nanofiber Membrane

The PVA-*co*-PE nanofiber membrane was immersed into a 3% v/v solution of BIBB (ATRP initiator) in toluene for 1 h at 25 °C. Then, the nanofiber membrane was thoroughly rinsed with toluene and ethanol. The nanofiber membrane activated by BIBB was obtained to initiate the polymerization of SBMA.

Grafting of the Zwitterionic SBMA onto the Surface of the Nanofiber Membrane

CuBr (1 mmol), bpy (1 mmol), and the BIBB-activated nanofiber membrane (0.2 g) were put into the reaction container with nitrogen protection. After 0.5 h, a mixed solution of methanol (38 mL), deionized water (38 mL), and SBMA (3.8 mmol) was infused into the reaction container, and the container was shaken for 6 h at 25 °C in a shaking mixer at 150 rpm. The nanofiber membrane was then thoroughly rinsed with ethanol, phosphate-buffered solution (PBS), and deionized water to remove the free polymer and all other excess reagents. The PSBMA-functionalized nanofiber membrane was dried at room temperature. A total synthesis diagrammatic sketch is shown in Scheme 1.

Characterization

The chemical structures of the pristine nanofiber membrane, surface-activated nanofiber membrane, and zwitterionic nanofiber membrane were characterized by ATR–FTIR spectroscopy (Tensor 27, Bruker). The surface element contents of each membrane were detected by XPS (VG Multilab 2000, Thermo). The surface morphologies of the nanofiber membranes were examined with a Hitachi X-650 scanning electron microscope. The contact angles of the pristine, surface-activated, and PSBMA-functionalized PVA-*co*-PE nanofiber membranes with water were measured by contact angle goniometry (KRÜSS, Germany). The concentration of the residual proteins was

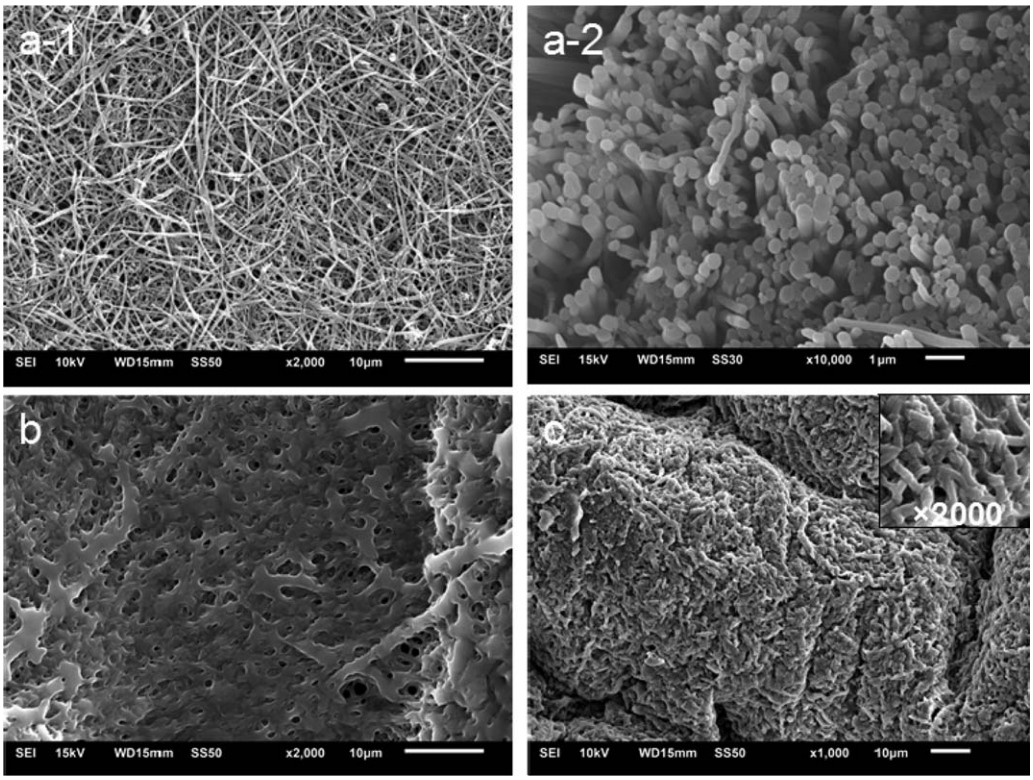

Figure 1. SEM images of the (a-1) surface of the pristine PVA-*co*-PE nanofiber membrane, (a-2) sectional morphology of the pristine PVA-*co*-PE nanofiber membrane, (b) surface of the BIBB-activated PVA-*co*-PE nanofiber membrane, and (c) surface of the zwitterionic PVA-*co*-PE nanofiber membrane.

measured on a Shimadzu UV-2700 ultraviolet–visible (UV–vis) spectrophotometer.

The grafting degree was defined as follows:

$$\text{Grafting degree} = (W_a - W_b)/W_b \times 100\%$$

where W_a and W_b are the weights of the nanofiber membrane after and before grafting with SBMA, respectively.[23]

Assessment of the Resistance to Bacterial Adsorption

The resistance to bacterial adsorption of the PSBMA-functionalized nanofiber membranes was evaluated by a revised absorption method. *E. coli* was the test organism;[24,25] it was cultured for 24 h at 37 °C on an agar plate to be purified. Several typical colonies were transferred to sterilized nutrient broth and incubated for 12 h at the same temperature. The resulting colonies were counted, and the *E. coli* concentration was expressed as colony forming units per milliliter.[26] The concentration of bacteria was adjusted to between 1×10^5 and 3×10^5 cfu/mL. The *E. coli* suspension was diluted 250 times with aseptic water and then brought up for 3 h. The suspension (0.2 mL) was pipetted and uniformly dispersed onto the sterilized nanofiber membranes (foursquare with sides of 1 cm), which was then covered with a clean microscope slide. The fabric samples with *E.coli* were then cultured in an incubator for 7 h at 37 °C. Then, the samples were washed thoroughly with nonorganism water to remove the bacteria not attached onto the surface of the membranes. The membranes were put into containers with sterilized water and stirred with a shaking mixer for 15 min. The *E. coli* attached to the membranes was thoroughly eluted. The eluent was diluted 100, 1000, and 10,000 times. Each eluent (10 μL) was coated onto agar and incubated overnight at 37 °C. The pristine PVA-*co*-PE nanofiber membrane was used for comparison. The resistance to bacterial adsorption was defined as follows:

$$\text{Resistance} = (1 - V_1/V_2) \times 100\%$$

where V_1 and V_2 are the average number of the bacterial colony of the zwitterionic polymer-functionalized nanofiber membrane and the pristine membrane, respectively.

Assessment of the Resistance to Nonspecific Protein Adsorption

BCA was used to measure the adsorption of BSA onto the surfaces covered with PSBMA. The PA6 substrate, the pristine nanofiber membrane, and PSBMA-functionalized PVA-*co*-PE nanofiber membrane were each put onto a plate and equilibrated with PBS solution for 3 h in a shaking mixer. The substrate and nanofiber membranes were then immersed in 10 mL of a BSA solution (500 μg/mL in PBS) and incubated at 37 °C for 2 h. The membranes were then rinsed with PBS solution three times. The concentration of the residual proteins was determined by a BCA method at 562 nm with a UV–vis spectrophotometer. Triplicate parallel measurements were carried out.

RESULTS AND DISCUSSION

Morphologies of the PVA-*co*-PE Nanofiber Membranes

The morphologies of the pristine, surface-activated and PSBMA-functionalized PVA-*co*-PE nanofiber membranes were investigated by SEM, and the images are shown in Figure 1. The surface topography of the pristine PVA-*co*-PE nanofiber

Figure 2. Contact angle measurements of the (a) pristine PVA-*co*-PE nanofiber membrane, (b) BIBB-activated PVA-*co*-PE nanofiber membrane, and (c) PSBMA-functionalized PVA-*co*-PE nanofiber membrane.

membrane is shown in Figure 1(a-1); it displayed a well-defined nanofibrous but randomly distributed and loose morphology. It was proven by the sectional morphology shown in Figure 1(a-2) that the pristine nanofibers were circular. Moreover, the diameter distribution of nanofibers was narrow. Figure 1(b) shows that the surface activation of the nanofibrous membrane with BIBB seemed to cause slight swelling. This was ascribed to the fact that the surface activation was carried out in toluene and the change in the surface chemical structure could lead to a morphological change and the nanofibers uniting together. Therefore, the surface-activated nanofibers became thicker than the pristine ones. However, the nanofibers, after being functionalized with SBMA, as shown in Figure 1(c), became shorter and closely entwisted to appear like a stacked fishing net. The appearance of short, wormlike nanofibers might have been caused by the formation of polymer brushes of PSBMA on the surface of the nanofibers.

Wetting Property of the PVA-*co*-PE Nanofiber Membranes

The wetting properties of the pristine, BIBB-activated, and PSBMA-functionalized PVA-*co*-PE nanofiber membranes were evaluated by the measurement of the water contact angles, and the results are shown in Figure 2. As shown in Figure 2(a), the contact angle of the surface of the pristine PVA-*co*-PE nanofiber membrane was low at 27° because of the presence of massive hydroxyl groups. The hydrophobic carbonyl and bromine groups were introduced onto the surface of the PVA-*co*-PE nanofiber membrane after the activation of BIBB, and this led to a sharp increase in the contact angle from 27 to 75°, as shown in Figure 2(b). However, as shown in Figure 2(c), we observed that the water contact angle of the nanofiber membrane decreased significantly to 1° after the membrane was grafted with PSBMA, and this value was even lower than that of the pristine membrane. This indicated that hydration formed between the zwitterionic groups and water and that the zwitterionic surface was more hydrophilic than that of the pristine membrane. A strongly hydrophilic surface is beneficial for resistance to the adsorption of organisms onto materials.[27,28]

Characterization of the Chemical Structures of the PVA-*co*-PE Nanofiber Membranes

The surface chemical structures of the pristine, BIBB-activated, and PSBMA-functionalized PVA-*co*-PE nanofiber membranes were investigated by ATR–FTIR spectroscopy, as shown in Figure 3. For the pristine PVA-*co*-PE nanofiber membrane, the absorption peaks at 1327 and 1455 cm^{-1} were assigned to the bending vibrations of the C—H bond.[17] The peak at 1008 cm^{-1} was attributed to the C—O bond from the hydroxyl group.[29] Compared with the ATR–FTIR spectrum of the pristine nanofiber membrane shown in Figure 3(a), the spectrum of the BIBB-activated PVA-*co*-PE nanofiber membrane demonstrated new characteristic absorption peaks at 1725, 1284, and

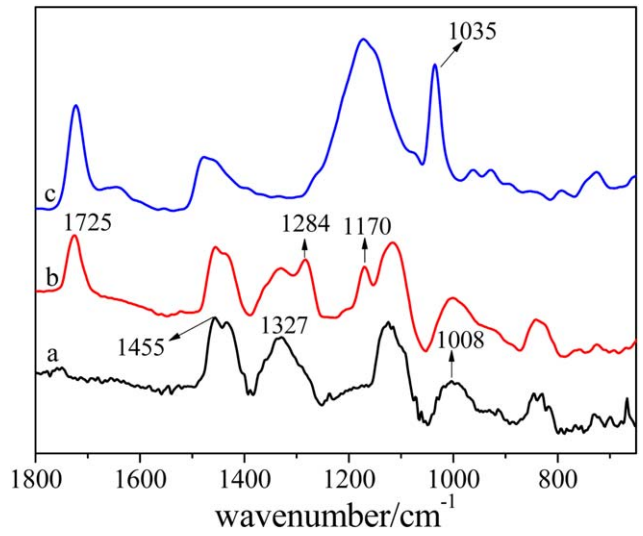

Figure 3. ATR–FTIR spectra of the (a) pristine PVA-*co*-PE nanofiber membrane, (b) BIBB-activated PVA-*co*-PE nanofiber membrane, and (c) PSBMA-functionalized PVA-*co*-PE nanofiber membrane. [Color figure can be viewed in the online issue, which is available at wileyonlinelibrary.com.]

1170 cm^{-1}, as indicated in Figure 3(b). The peaks were assigned to the carbonyl group (—C═O—), methyl group (—CH_3), and C—O bond, respectively, in BIBB.[30,31] Figure 3(c) shows the ATR–FTIR spectrum of the PSBMA-functionalized PVA-*co*-PE nanofiber membrane. We observed that a new absorption peak at 1035 cm^{-1} existed in the spectrum; this was ascribed to the symmetric stretching vibrations of sulfonate groups.[15,32]

The elemental contents on the surfaces of the pristine, BIBB-activated, and PSBMA-functionalized PVA-*co*-PE nanofiber membranes were analyzed by XPS. The detailed spectra from XPS and elemental contents of different nanofiber membranes are shown in Figure 4 and Table I. From the comparison given in Figure 4(a,b), we calculated that the contents of carbon and

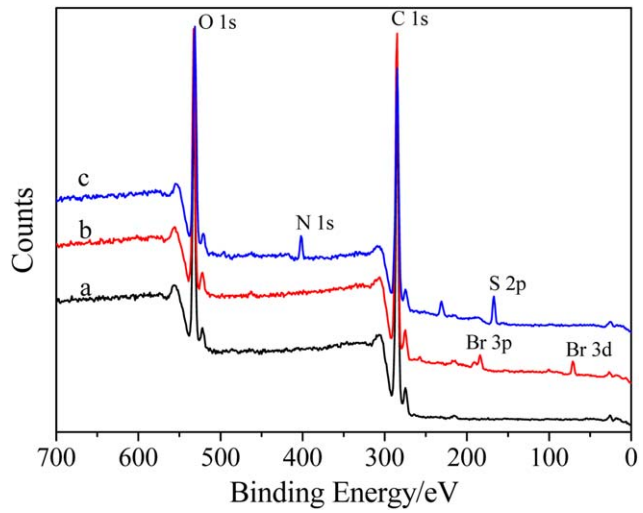

Figure 4. XPS spectra of the (a) pristine PVA-*co*-PE nanofiber membrane, (b) BIBB-activated PVA-*co*-PE nanofiber membrane, and (c) PSBMA-functionalized PVA-*co*-PE nanofiber membrane. [Color figure can be viewed in the online issue, which is available at wileyonlinelibrary.com.]

Table I. Chemical Element Contents of the Pristine, BIBB-Activated, and PSBMA-Functionalized PVA-*co*-PE Nanofiber Membranes

	Elemental composition (%)				
Nanofiber membrane	Carbon	Oxygen	Bromine	Nitrogen	Sulfur
Pristine	78.62	21.38	—	—	—
BIBB-activated	78.34	20.93	0.44	—	—
PSBMA-functionalized	69.98	23.18	—	2.96	3.88

Table II. Grafting Degrees of the Functionalized PVA-*co*-PE Nanofiber Membranes

Nanofiber membrane	Overall grafting degree (%)[a]	Grafting degree (%)[b]
BIBB-activated	0.83	0.83
PSBMA-functionalized	33.8	51.48

[a] The overall grafting degree was calculated according to the weight of the virgin nanofiber membranes.
[b] The grafting degree at each step was calculated according to the weight of the nanofiber membranes before and after each step.

oxygen slightly decreased after BIBB was grafted onto the surface of the nanofiber membranes. Moreover, as shown in Figure 4(b), the additional characteristic peaks for bromine (Br 3p = 184 eV and Br 3d = 70 eV) were observed; this indicated that the ATRP initiator was covalently linked to the surface of the nanofiber membrane.[33,34] The weight ratio of bromine was 0.44%. When the ATRP reaction was complete, the contents of carbon and oxygen decreased remarkably, and the peak for bromine disappeared, whereas peaks for nitrogen and sulfur occurred at 402 and 167 eV. The contents were 2.96 and 3.88%, respectively. This indicated the PSBMA was successfully grafted onto the surface of the PVA-*co*-PE nanofiber membrane.[14,35] The grafting degree of the functionalized PVA-*co*-PE nanofiber membranes in each step were calculated and are presented in Table II. The grafting degree of the BIBB-activated nanofiber membrane was 0.83%, and this was attributed to the high reactivity of BIBB, even when a small amount was used. The PSBMA was greatly conjugated onto the BIBB-activated nanofiber membrane with a grafting degree of 51.48%; this indicated that polymer chains were formed on the nanofiber membrane.

Resistance to Bacterial Adsorption

To combat the formation of biofilm, which can potentially affect most medical devices, including wound dressings, it is crucial to stop or reduce initial bacterial adhesion onto these surfaces. Hydrophilic uncharged surfaces, such as poly(ethylene oxide) and PSBMA, have shown great resistance to bacterial attachment.[36,37]

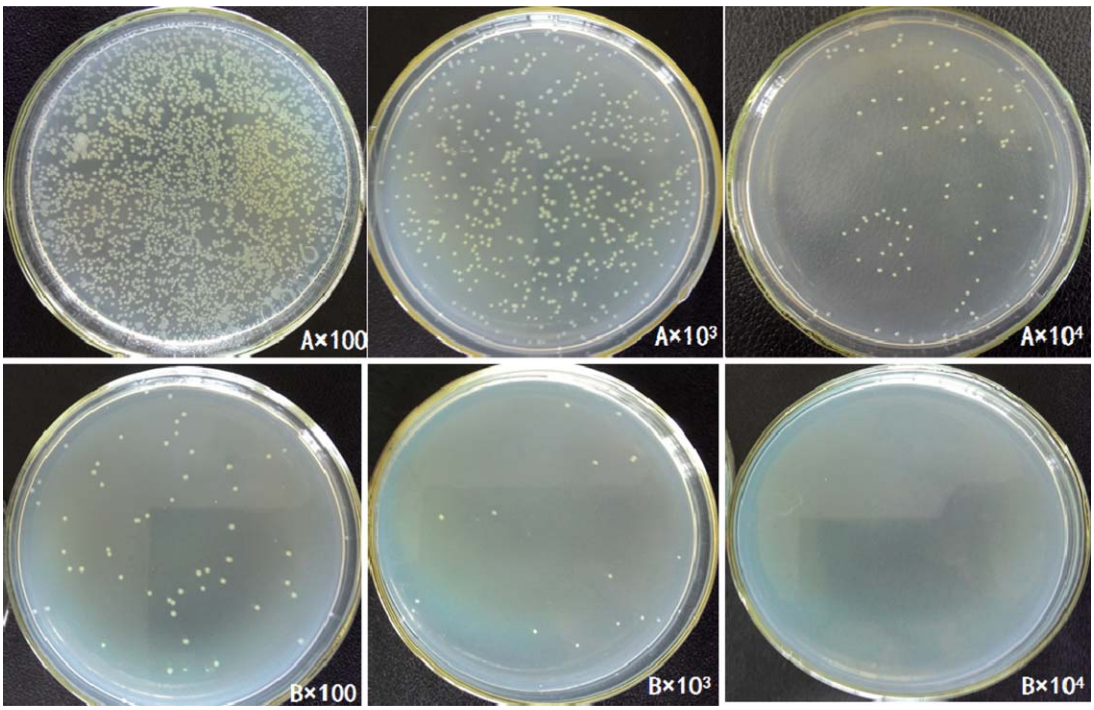

Figure 5. Photographs of the residual *E. coli* bacteria growing on agar sterilized with the (A) pristine nanofiber membrane and (B) PSBMA-functionalized nanofiber membrane. The eluent was diluted 100, 1000, and 10,000 times. [Color figure can be viewed in the online issue, which is available at wileyonlinelibrary.com.]

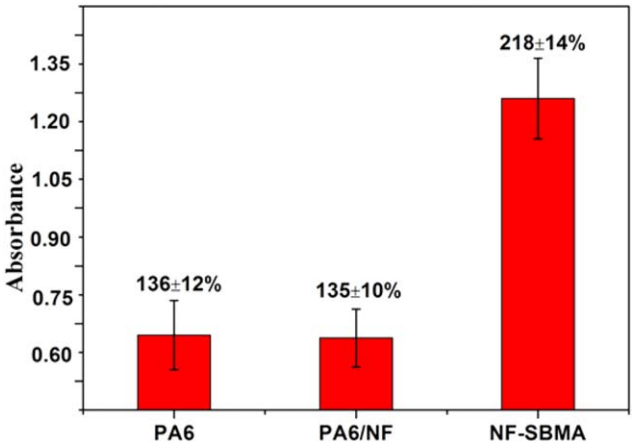

Figure 6. Absorbance of the residual BSA after absorption by different membranes. The data at the top of the columns are the relative concentration values (percentages) presented as means and standard deviations. The PA6 substrate, PVA-*co*-PE nanofiber membrane (PA6/NF), and PSBMA-functionalized nanofiber membrane (NF–SBMA) were incubated in BSA at 37 °C for 2 h. [Color figure can be viewed in the online issue, which is available at wileyonlinelibrary.com.]

The pristine nanofiber membrane without functionalization was used as the contrast sample in the evaluation of the resistance to bacteria attachment of the PSBMA-functionalized nanofiber membrane. Figure 5 shows the photos for the residual *E. coli* bacteria growing on agar, which was sterilized by the pristine and PSBMA-functionalized nanofiber membranes. As shown in Figure 5, it was obvious that the optimal dilution factor of the pristine was 10,000 times; at this dilution, the bacterial amount was appropriate. The optimal factor for the functional nanofiber membrane alternated between 1000 and 10,000 times. Compared with the pristine nanofiber membrane, the bacterial amount sharply declined in the functionalized membrane; this indicated that the PSBMA-functionalized nanofiber membrane possessed a decent resistance to bacterial adsorption. Moreover, zwitterionic moieties favored water entrapment, as shown earlier by the improved surface hydrophilicity [Figure 2(c)]. A water film formed surrounding the PSBMA brushes and, therefore, prevented bacteria from adhering to the surfaces.[38] In addition, the antibacterial adsorption rate was 99.5% according to the previous formula, which illustrated that the amphiphilic nanofiber membrane possessed excellent properties of antibacterial adsorption.

Nonspecific Adsorption of Protein

The nonspecific adsorption of protein on the three surfaces was determined by the BCA method, and the absorbance of residual protein was characterized by UV–vis spectroscopy. Figure 6 shows the absorbance of the residual protein from the BSA solution after it was adsorbed by the PA6 substrate, PA6/nanofiber membrane, and PSBMA-functionalized nanofiber membrane. As shown in Figure 6, the residual concentration of protein after it was adsorbed by the PSBMA-functionalized membrane was about 218 μg/mL, whereas the residual concentration of the two contrasts were nearly two-thirds of this. We believe that zwitterionic surface could form a hydration layer via electrostatic interaction and hydrogen bonds; this resulted in the binding of a significant amount of water. As a result, it led to a strong repelling force, which kept nonspecific proteins at a distance or made nonspecific proteins come into contact with the surface in a reverse manner without a significant conformation change.[39] As a result, the PSBMA-functionalized nanofiber membrane resisted the nonspecific adsorption of protein. Moreover, the PVA-*co*-PE nanofiber could be prepared on a large scale in our group, and the nonwoven nanofiber membrane could be prepared more easily than other commercial membranes by our method. Therefore, there is potential to prepare these membranes in quantity for resistance to the adsorption of bacteria and protein.

CONCLUSIONS

Zwitterionic PSBMA was immobilized onto the surface of PVA-*co*-PE nanofiber membranes via ATRP to fabricate an antibacterial and biocompatible surface. ATR–FTIR spectroscopy and XPS analysis confirmed successful activation with BIBB and subsequent covalent binding of PSBMA onto PVA-*co*-PE nanofiber membranes. The immobilization of PSBMA onto the surface of the nanofiber membrane significantly improved the hydrophilicity and wetting properties of the membrane; this consequently increased its ability to form a hydration layer. The assessment of the resistance to bacterial adsorption proved that the PSBMA-functionalized PVA-*co*-PE nanofiber membrane possessed an excellent antibacterial adsorption rate of 99.5%. Moreover, the zwitterionic nanofiber membrane, which was more biocompatible, had better resistance to the nonspecific adsorption of protein. Therefore, this study afforded us with a convenient and promising method for preparing a new kind of antibacterial adsorption and low-fouling material, which could be used in many fields.

ACKNOWLEDGMENTS

The authors are grateful for the financial support of the National Natural Science Foundation of China (contract grant numbers 51403166, 51473129, and 51273152), the 863 Special Project on Functional Nanomaterials (contract grant number 2013AA031802), and the Program for New Century Excellent Talents in University (contract grant number NCET-12-0711). They also acknowledge the financial support of the Plan for the Scientific and Technological Innovation Team of Excellent Middle-Aged and Young Team from the Educational Commission of Hubei Province of China (contract grant number T201408) and the Nature Science Foundation of Hubei Province (contract grant number 2014CFB759). Financial support from the Science and Technology Research Project of the Educational Commission of Hubei Province (contract grant number Q20161603) is also acknowledged.

REFERENCES

1. Park, J.; Lakes, R. S. Biomaterials: An Introduction; Springer Science & Business Media: Berlin, **2007**.
2. Nair, L. S.; Laurencin, C. T. *Prog. Polym. Sci.* **2007**, *32*, 762.
3. Ratner, B. D. *Biomaterials* **2007**, *28*, 5144.
4. Kawabata, N.; Inoue, T.; Tomita, H. *Epidemiol. Infect.* **1992**, *108*, 123.

5. Muñoz-Bonilla, A.; Fernández-García, M. *Prog. Polym. Sci.* **2012**, *37*, 281.
6. Seo, J.-H.; Matsuno, R.; Konno, T.; Takai, M.; Ishihara, K. *Biomaterials* **2008**, *29*, 1367.
7. Wei, Q.; Becherer, T.; Angioletti-Uberti, S.; Dzubiella, J.; Wischke, C.; Neffe, A. T.; Lendlein, A.; Ballauff, M.; Haag, R. *Angew. Chem. Int. Ed.* **2014**, *53*, 8004.
8. Díaz Blanco, C.; Ortner, A.; Dimitrov, R.; Navarro, A.; Mendoza, E.; Tzanov, T. *ACS Appl. Mater. Interfaces* **2014**, *6*, 11385.
9. Li, Q.; Imbrogno, J.; Belfort, G.; Wang, X. L. *J. Appl. Polym. Sci.* **2015**, *132*, DOI: 10.1002/app.41781
10. Colilla, M.; Martínez-Carmona, M.; Sánchez-Salcedo, S.; Ruiz-González, M. L.; González-Calbet, J. M.; Vallet-Regí, M. *J. Mater. Chem. B* **2014**, *2*, 5639.
11. Chen, S.; Chen, S.; Jiang, S.; Mo, Y.; Luo, J.; Tang, J.; Ge, Z. *Colloids Surf. B* **2011**, *85*, 323.
12. Mo, F.; Ren, H.; Chen, S.; Ge, Z. *Mater. Lett.* **2015**, *145*, 174.
13. Ladd, J.; Zhang, Z.; Chen, S.; Hower, J. C.; Jiang, S. *Biomacromolecules* **2008**, *9*, 1357.
14. Li, M.-Z.; Li, J.-H.; Shao, X.-S.; Miao, J.; Wang, J.-B.; Zhang, Q.-Q.; Xu, X.-P. *J. Membr. Sci.* **2012**, *405*, 141.
15. Zhao, Y.-H.; Wee, K.-H.; Bai, R. *J. Membr. Sci.* **2010**, *362*, 326.
16. Hu, R.; Li, G.; Jiang, Y.; Zhang, Y.; Zou, J.-J.; Wang, L.; Zhang, X. *Langmuir* **2013**, *29*, 3773.
17. Lu, Y.; Wu, Z.; Li, M.; Liu, Q.; Wang, D. *React. Funct. Polym.* **2014**, *82*, 98.
18. Li, M.; Xue, X.; Wang, D.; Lu, Y.; Wu, Z.; Zou, H. *Desalination* **2013**, *329*, 50.
19. Xia, M.; Liu, Q.; Zhou, Z.; Tao, Y.; Li, M.; Liu, K.; Wu, Z.; Wang, D. *J. Power Sources* **2014**, *266*, 29.
20. Li, M.; Wu, Z.; Luo, M.; Wang, W.; Chang, K.; Liu, K.; Liu, Q.; Xia, M.; Wang, D. *Cellulose* **2015**, *22*, 1.
21. Wang, D.; Liu, N.; Xu, W.; Sun, G. *J. Phys. Chem. C* **2011**, *115*, 6825.
22. Wang, D.; Sun, G.; Chiou, B. S. *Macromol. Mater. Eng.* **2007**, *292*, 407.
23. Huang, J.; Wang, D.; Lu, Y.; Li, M.; Xu, W. *RSC Adv.* **2013**, *3*, 20922.
24. Rizzo, L.; Sannino, D.; Vaiano, V.; Sacco, O.; Scarpa, A.; Pietrogiacomi, D. *Appl. Catal. B* **2014**, *144*, 369.
25. Matai, I.; Sachdev, A.; Dubey, P.; Kumar, S. U.; Bhushan, B.; Gopinath, P. *Colloids Surf. B* **2014**, *115*, 359.
26. Stauber, C.; Elliott, M.; Koksal, F.; Ortiz, G.; DiGiano, F.; Sobsey, M. *Water Sci. Technol.* **2006**, *54*, 1.
27. Shao, Q.; He, Y.; White, A. D.; Jiang, S. *J. Phys. Chem. B* **2010**, *114*, 16625.
28. Chen, S.; Li, L.; Zhao, C.; Zheng, J. *Polymer* **2010**, *51*, 5283.
29. Zhu, J.; Sun, G. *React. Funct. Polym.* **2012**, *72*, 839.
30. Bao, L.; Chen, Y.; Zhou, W.; Wu, Y.; Huang, Y. *J. Appl. Polym. Sci.* **2011**, *122*, 2456.
31. Liu, Y.-L.; Chen, M.-H.; Hsu, K.-Y. *React. Funct. Polym.* **2009**, *69*, 424.
32. Li, J.-H.; Li, M.-Z.; Miao, J.; Wang, J.-B.; Shao, X.-S.; Zhang, Q.-Q. *Appl. Surf. Sci.* **2012**, *258*, 6398.
33. Zhu, B.; Edmondson, S. *Polymer* **2011**, *52*, 2141.
34. Teixeira, F.; Popa, A. M.; Guimond, S.; Hegemann, D.; Rossi, R. M. *J. Appl. Polym. Sci.* **2013**, *129*, 636.
35. Puniredd, S. R.; Jayaraman, S.; Gandhimathi, C.; Ramakrishna, S.; Venugopal, J. R.; Yeo, T. W.; Guo, S.; Quintana, R.; Jańczewski, D.; Srinivasan, M. P. *J. Colloid Interface Sci.* **2015**, *448*, 156.
36. Cheng, G.; Zhang, Z.; Chen, S.; Bryers, J. D.; Jiang, S. *Biomaterials* **2007**, *28*, 4192.
37. Cunliffe, D.; Smart, C.; Alexander, C.; Vulfson, E. *Appl. Environ. Microb.* **1999**, *65*, 4995.
38. Fraga, H.; Fernandes, D.; Novotny, J.; Fontes, R.; Esteves da Silva, J. C. *ChemBioChem* **2006**, *7*, 929.
39. Fraga, H.; Esteves da Silva, J. C.; Fontes, R. *ChemBioChem* **2004**, *5*, 110.